NeuroImage: Clinical 24 (2019) 102046

Contents lists available at ScienceDirect

NeuroImage: Clinical

journal homepage: www.elsevier.com/locate/ynicl

EEG time signature in Alzheimer´s disease: Functional brain networks falling apart

Una Smailovic[a,*], Thomas Koenig[b], Erika J Laukka[c,d], Grégoria Kalpouzos[c], Thomas Andersson[e], Bengt Winblad[f], Vesna Jelic[g]

[a] Karolinska Institute, Department of Neurobiology, Care Sciences and Society, Division of Clinical Geriatrics, Huddinge, Sweden
[b] Translational Research Center, University Hospital of Psychiatry, University of Bern, Bern, Switzerland
[c] Department of Neurobiology, Care Sciences and Society, Aging Research Center, Karolinska Institute and Stockholm University, Stockholm, Sweden
[d] Stockholm Gerontology Research Center, Stockholm, Sweden
[e] Department of Clinical Neurophysiology, Karolinska University Hospital, Huddinge, Sweden
[f] Karolinska Institute, Department of Neurobiology, Care Sciences and Society, Division of Neurogeriatrics, Solna, Sweden and Karolinska University Hospital, Department of Geriatrics, Huddinge, Sweden
[g] Karolinska Institute, Department of Neurobiology, Care Sciences and Society, Division of Clinical Geriatrics and Karolinska University Hospital, Memory Clinic, Huddinge, Sweden

ARTICLE INFO

Keywords:
Alzheimer's disease
Biomarkers
Electroencephalography
Functional microstates
Cerebrospinal fluid

ABSTRACT

Spontaneous mental activity is characterized by dynamic alterations of discrete and stabile brain states called functional microstates that are thought to represent distinct steps of human information processing. Electroencephalography (EEG) directly reflects functioning of brain synapses with a uniquely high temporal resolution, necessary for investigation of brain network dynamics. Since synaptic dysfunction is an early event and best correlate of cognitive status and decline in patients along Alzheimer's disease (AD) continuum, EEG microstates might serve as valuable early markers of AD. The present study investigated differences in EEG microstate topographies and parameters (duration, occurrence and contribution) between a large cohort of healthy elderly (n = 308) and memory clinic patients: subjective cognitive decline (SCD, n = 210); mild cognitive impairment (MCI, n = 230) and AD (n = 197) and how they correlate to conventional cerebrospinal fluid (CSF) markers of AD. Four most representative microstate maps assigned as classes A, B (asymmetrical), C and D (symmetrical) were computed from the resting state EEGs since it has been shown previously that this is sufficient to explain most of the resting state EEG data. Statistically different topography of microstate maps were found between the controls and the patient groups for microstate classes A, C and D. Changes in the topography of microstate class C were associated with the CSF Aβ42 levels, whereas changes in the topography of class B were linked with the CSF p-tau levels. Gradient-like increase in the contribution of asymmetrical (A and B) and gradient-like decrease in the contribution of symmetrical (C and D) maps were observed with the more severe stage of cognitive impairment. Our study demonstrated extensive relationship of resting state EEG microstates topographies and parameters with the stage of cognitive impairment and AD biomarkers. Resting state EEG microstates might therefore serve as functional markers of early disruption of neurocognitive networks in patients along AD continuum.

AD	Alzheimer's disease
CSF	cerebrospinal fluid
EEG	electroencephalography
FDG-PET	fluorodeoxyglucose-PET
fMRI	functional magnetic resonance imaging
GFS	Global Field Synchronization
GFP	Global Field Power
HC	healthy elderly controls
ICA	independent component analysis
MCI	mild cognitive impairment
MMSE	Mini-Mental State Examination
PLI	Phase Lag Index
qEEG	quantitative electroencephalography
SCD	subjective cognitive decline

* Corresponding author at: Division of Clinical geriatrics, Department of NVS, Karolinska Institute, 141 83 Huddinge, Sweden.
E-mail address: una.smailovic@ki.se (U. Smailovic).

https://doi.org/10.1016/j.nicl.2019.102046
Received 19 May 2019; Received in revised form 2 October 2019; Accepted 17 October 2019
Available online 18 October 2019

SNAC-K Swedish National study on Aging and Care – Kungsholmen
TANCOVA topographic analysis of covariance
TANOVA topographic analysis of variance

1. Introduction

How the brain integrates large-scale distributed neural activity into coherent cognitive processes is one of the ongoing puzzles in cognitive neuroscience. Many studies using different functional imaging modalities have investigated and confirmed functional interaction of extensive neuronal populations organized to perform cognitive functions in the form of neurocognitive networks (Varela et al., 2001; Bressler and Menon, 2010). Conjointly, they revealed that human brain activity constitutes of functionally connected brain areas that are synchronously active during the task-absent resting state (Raichle et al., 2001). Stimulus-independent spontaneous mental activity is therefore a result of global intrinsic well-organized brain activity during rest (Raichle, 2010).

Impaired functional connectivity has been repeatedly reported in various neuropsychiatric disorders (He et al., 2007; Seeley et al., 2009; Bressler and Menon, 2010). Alzheimer's disease (AD) is of particular interest since it is characterized by disturbance of higher cortical functions such as memory, comprehension, learning capacity, language, etc. Moreover, it is accompanied by the impairment of thinking and reasoning as well as with reduction in the flow of ideas (World Health Organization, 1992). Dementia in AD evolves on a continuum consisting of subjective cognitive decline (SCD) as the first symptomatic and mild cognitive impairment (MCI) as the subsequent prodromal stage of the disease (Jessen et al., 2010; Jessen et al., 2014). Preclinical and clinical stages of AD have already been recognized as "disconnection syndromes" since numerous functional magnetic resonance imaging (fMRI) and quantitative electroencephalography (qEEG) studies have shown disturbances in resting state functional connectivity of different brain regions in the referred patient groups (Leuchter et al., 1992; Jelic et al., 1996; Li et al., 2002; Koenig et al., 2005; Damoiseaux, 2012; Badhwar et al., 2017; Smailovic et al., 2018). Widespread distribution of neuropathological hallmarks in the brain, such as amyloid plaques and neurofibrillary tangles might subtend disruptions in the large-scale neurocognitive networks. Besides, it has already been postulated that neurodegeneration, neuronal and synaptic loss and dysfunction might lead to the loss of structural and functional integrity of the long cortico-cortical projections, which gives rise to the clinical symptoms of AD (Morrison et al., 1996; Badhwar et al., 2017; Smailovic et al., 2018). Therefore, diagnostic modalities that have a capability to detect disruptions in spontaneous mental processes in subsecond time dimension, i.e. disturbances in large-scale resting state neural networks, are candidate markers of early AD.

EEG has long been proven to be a valuable method for investigation of the brain resting states as it directly mirrors brain synaptic activity, i.e. summated excitatory and inhibitory postsynaptic potentials, with a uniquely high temporal resolution (Michel, 2009). Conventional qEEG analysis in the frequency domain, such as power spectra analysis together with the novel qEEG measures of functional connectivity involving global field synchronization (GFS) and phase lag index (PLI) have already been proven to correlate with the stage of cognitive impairment (Huang et al., 2000; Park et al., 2008; Engels et al., 2015) and AD molecular biomarkers (Smailovic et al., 2018). However, the referred frequency analyses integrate EEG recording over seconds and therefore entail loss of temporal resolution. Employing multichannel EEG analysis in the time domain with the millisecond time resolution might therefore provide a valuable tool for an investigation of the dynamics of resting state neurocognitive networks.

EEG recording can be directly visualized by a single scalp field map, i.e. color-dependent plot of potentials recorded across all electrodes sites. These maps or topographies of electric fields vary throughout recording time as they are generated by the ensemble of all active neural networks in the brain at one given moment in time. Therefore, temporal organization of the large-scale neural networks can be analyzed using topographies of electric fields measured at the level of the scalp. Previous studies revealed two notable properties of the resting state EEG time domain analysis. First, these arrangements of electric fields remain quasi-stable for a certain length of time before a sudden transition into the new arrangement (Lehmann et al., 1987). Referred periods of stabile topographies of electric potentials do not overlap in time and last around 60–120 ms (Lehmann et al., 1987; Koenig et al., 2002; Michel and Koenig, 2018) which is compatible with the resolution of the human information processing (Efron, 1970). They were proposed to represent elementary and momentary unit of thoughts as the "atoms of thoughts" and were named functional microstates (Lehmann et al., 1998; Lehmann et al., 2010). Second, microstate topographies are notably similar across EEGs of different subjects. Only four distinct alternating maps are sufficient to explain most of the topographical variance of the resting state EEG data (Pascual-Marqui et al., 1995; Koenig et al., 2002). These microstate topographies were named class (map) A, B (asymmetrical), C and D (symmetrical). Previous studies employing resting-state fMRI and EEG modalities have provided evidence for the temporal correlation between the occurrence of the specific microstate map and the activity of a particular resting state network of the brain (Britz et al., 2010; Musso et al., 2010; Yuan et al., 2012). In more detail, Britz et al. reported association of the microstate maps A and B with auditory and visual and microstate maps C and D with saliency and attention networks (Britz et al., 2010). Another study that involved EEG source localization technique found that cortical generators of neuronal electric activity that give rise to EEG microstates correspond to the parts of the default mode network (DMN) (Pascual-Marqui et al., 2014). The above findings motivated EEG microstate investigations in patients with AD, since dysfunction of the referred resting state networks have been repeatedly reported in cognitively impaired individuals (Sorg et al., 2007; Li et al., 2012; Verma and Howard, 2012; Hafkemeijer et al., 2015; Wang et al., 2015; Badhwar et al., 2017; Mascali et al., 2018).

Several studies have reported decreased microstate duration in patients with different stages of cognitive impairment and AD (Dierks et al., 1997; Strik et al., 1997; Stevens and Kircher, 1998). Conversely, longer overall microstate duration in patients with AD compared to healthy elderly has also been reported (Ihl et al., 1993). Although findings originated from small-scale clinical studies and involved outdated analytical methodology based on two-dimensional map descriptors, they indicated a relationship between cognitive status and microstate parameters. However, thorough investigation of the microstate topographies and parameters and their relationship to the molecular markers of AD neuropathology in a well-defined memory clinic cohort have not been conducted so far.

In accordance with the growing need for the early and reliable functional state and trait markers of AD as well as noninvasive outcome measures in clinical trials, the aim of the present study was to investigate the relationship of EEG microstates with the cognitive status and conventional AD CSF biomarkers. We hypothesized that both microstate topographies and parameters are altered in the cognitively impaired patients compared to healthy elderly controls and that these changes are associated with AD-like CSF biomarker profile. The study population included over 600 memory clinic patients with wide spectra of cognitive impairment and 300 healthy elderly controls.

2. Material and methods

2.1. Study population

The present study included 308 healthy elderly controls recruited as part of the Swedish National study on Aging and Care in Kungsholmen, Stockholm (SNAC-K) and 637 cognitively impaired patients from the Memory Clinic, Karolinska University Hospital Huddinge. The SNAC-K

Table 1
Demographics of the study population and CSF biomarker values of the patient group.

	Controls	SCD	MCI	AD
Number	308	210	230	197
Sex ratio (males/females)	121/187	79/131	109/121	72/125
Age (years)	71.6 ± 8.8 [b,c,d] (60–93)	60.0 ± 6.1 [b,e,f] (50–83)	65.9 ± 8.2 [c,e] (50–87)	67.8 ± 9.2 [d,f] (51–89)
Education (years)	14.4 ± 3.1 [b,c,d] (9–18)	13.3 ± 3.6 [b,e,f] (1–24.5)	12.1 ± 3.8 [c,e,g] (3–22)	11.1 ± 3.6 [d,f,g] (6–23)
MMSE[a]	29.3 ± 0.8 [b,c,d] (27–30)	28.7 ± 1.7 [b,e,f] (23–30)	27.3 ± 2.1 [c,e,g] (18–30)	23.0 ± 4.3 [d,f,g] (7–30)
CSF biomarkers				
CSF Aβ42 (ng/L)	-	916.9 ± 248.8 [e,f] (300–1650)	713.6 ± 271.7 [e,g] (229–1532)	500.9 ± 123.5 [f,g] (250–876)
CSF p-tau (ng/L)	-	52.4 ± 21.5 [e,f] (16–183)	62.7 ± 28.6 [e,g] (16–175)	91.5 ± 37.6 [f,g] (16–240)
CSF t-tau (ng/L)	-	256.3 ± 121.4 [e,f] (43–689)	363.6 ± 210.3 [e,g] (41–1140)	628.7 ± 309.5 [f,g] (103–1500)

Data are presented as means ± standard deviation. Kruskal–Wallis test; $p < 0.05$ for age, education, MMSE and all CSF biomarkers. Dunn–Bonferroni test for post-hoc comparisons. SCD = subjective cognitive decline, MCI = mild cognitive impairment, AD = Alzheimer's disease, MMSE = Mini Mental State Examination. [a] $n = 627$ for the memory clinic cohort (Controls = 308, SCD = 206, MCI = 228, AD = 193). [b] $p < 0.05$, Controls versus SCD; [c] $p < 0.05$, Controls versus MCI; [d] $p < 0.05$, Controls versus AD; [e] $p < 0.05$, SCD versus MCI; [f] $p < 0.05$, SCD versus AD; [g] $p < 0.05$, MCI versus AD.

study was approved by the Ethics Committee at Karolinska Institute and the Regional Ethical Review Board in Stockholm (Dnrs: 01-114, 04-929/3, Ö 26-2007). The involvement of the patients in the study was approved by the local ethical committee of the Karolinska University Hospital Huddinge (Dnr: 2011/1978-31/4). Informed written consent was obtained according to the Declaration of Helsinki from all participants. All patients had capacity to take a decision to donate the results of their routine assessments for the research purposes. Table 1. Presents the demographic characteristics of the study population (healthy elderly and memory clinic patients).

2.1.1. Healthy elderly controls (SNAC-K cohort)

SNAC-K is a population-based study that started in 2001 and recruited individuals ≥60 years of age living at home or in institutions. The participants were randomly selected from age-stratified groups in 6- (between 60 and 78 years) and 3-year intervals (> 81 years). All participants underwent extensive examination consisting of a social interview and assessment of physical functioning, a psychological test battery, self-administrated questionnaires and a comprehensive clinical assessment including geriatric and neurological examination together with laboratory tests. At baseline, a subsample of participants who were free from dementia underwent an extended biomedical assessment including structural MRI imaging and resting state EEG recordings. Depending on their age, the participants are re-examined every 6 (between 60 and 78 years) or every 3 years (> 78 years).

In total, 484 participants underwent resting state EEG recording but 308 were retained for the analyses following the exclusion criteria (121 males and 187 females, mean age 71.6, mean Mini-Mental State Examination (MMSE) score 29.3) (Table 1.). The exclusion criteria included (i) a baseline MMSE score lower than 27 points; (ii) decline in the MMSE of more than two points and/or a dementia diagnosis (DSM IV criteria) during the first 6 years of the follow-up; and (iii) presence of any major neurological and/or psychiatric disorder evidenced by the medical history or neuroradiological report.

2.1.2. Memory clinic cohort

The patient group consisted of 637 memory clinic referrals clinically diagnosed with SCD ($n = 210$) comparable to the Jessen et al. (2014), MCI ($n = 230$) according to Winblad et al. (2004) and AD ($n = 197$) according to ICD-10 criteria (World Health Organization, 1992). All patients underwent routine comprehensive clinical examination, neuropsychological testing, CSF sampling and resting state EEG recording at the baseline. The exclusion criteria together with the demographics and clinical data (Table 1) were previously described in more details in Smailovic et al. (2018).

2.2. CSF sampling and analysis

The patient groups involved in the present study underwent CSF sampling and conventional CSF biomarker analysis (Aβ42, p- and t-tau). CSF sampling was conducted in the morning by routine lumbar puncture procedure in the L3/L4 or L4 /L5 intervertebral space while the patient was sitting in an upright position. CSF samples were collected in polypropylene tubes, centrifuged at 1000rpm (10 minutes) in order to eliminate cells and insoluble material and stored at -70°C pending further analysis. CSF Aβ42, p-tau (threonine 181) and t-tau protein concentrations were analyzed with xMAP technology using the INNO-BIA AlzBio3 kit (Innogenetics, Ghent, Belgium) (Olsson et al., 2005). The cutoff values were Aβ42 > 550 ng/L, p-tau < 80 ng/L, and t-tau < 400 ng/L. The healthy individuals did not undergo lumbar puncture due to ethical constraints.

2.3. EEG recordings

The resting state EEG recordings of the healthy elderly (SNAC-K) and memory clinic cohorts share key features of the methodological setup. However, they were conducted in different clinical and/or research frameworks and their differences are therefore described separately below. Raw EEG recordings of both cohorts were further preprocessed and analyzed following the same methodological procedure.

2.3.1. EEG recordings of the healthy elderly controls

The subjects underwent resting-state EEG recordings on the Schwarzer EEG Natus Incorporated System by using Easy Caps with the placement of the 19 scalp electrodes, proven to be sufficient for reliable microstate analysis (Khanna et al., 2014), following the standard 10/20 system. The subjects had their eyes closed and their vigilant state has been monitored during spontaneous real-time EEG recording. In case of changes in the vigilant state (e.g. drowsiness), the subjects would receive an auditory warning sound. The sampling rate of the EEG recording was 256 Hz with the electrode impedance below 5 kΩ and band-pass filters between 0.5 Hz and 70 Hz.

2.3.2. EEG recordings of the memory clinic patients

The patient group underwent resting-state EEG recording on the Nervus System. The recording setup was identical to the one used in the healthy control group as noted above. Compatibility of two recording systems (Schwarzer Natus and Nervus) was checked by dummy signal generator recordings on both systems.

2.4. EEG microstate analysis

The preprocessing of the EEGs of both healthy elderly controls and memory clinic patients was conducted in Brain Vision Analyzer, version 2.0 software (Gilching, Germany). Eye movements and electrocardiographic artifacts were removed using independent component analysis (ICA) algorithm while remaining artifacts, periods of drowsiness, eyes open and other non-resting state vigilant states were removed by visual inspection. The average total length of the preprocessed EEG recording available for the further analysis was between 6 (healthy controls) and 11 min (patient groups).

Microstates analysis was performed on all the available segments of the preprocessed EEG data in MATLAB version R2017. The analysis followed well established procedure previously described in detail (Pascual-Marqui et al., 1995; Koenig et al., 2002). Functional microstates are defined as periods of stable electric field topographies that do no overlap in time and undergo sharp transitions into new topographical configurations (Lehmann et al., 1987). It has been previously shown that these topographies remain stable around the global field power (GFP) peaks and tend to change at the moments of the minimal GFP values (Michel, 2009). Therefore, topographies (maps) at the GFP peaks throughout the whole 2-20 Hz band-pass filtered EEG data were subjected to the modified *k*-means spatial cluster algorithm. Referred cluster analysis yielded four most representative microstate maps per participant, previously found to be optimal to explain most of the variance in the resting state EEG data (Koenig et al., 2002). Four individual microstate maps of all the healthy elderly subjects were further averaged in order to compute four average or grand mean microstate maps of the control group. The control's grand mean microstate maps were assigned as class A, B, C and D based on the similarity to the normative microstate maps available from the literature (Koenig et al., 2002). Finally, the four individual maps of all the subjects in the study (healthy controls and patients) were assigned as class A, B, C and D based on the similarity to the corresponding controls' grand mean microstate maps (Fig. 1) and were further used for the statistical analysis of their corresponding topographical differences.

The analysis of microstate parameters included computation of duration, occurrence and contribution of each microstate map in the EEG recording. Duration corresponds to the continuous period within which particular microstate class is active and presumably reflects stability of the underlying active brain networks. Occurrence corresponds to the average number of appearance of each microstate class per second and may resemble the tendency of the underlying brain networks to become activated. Contribution is a microstate parameter defined as a percentage of the total time occupied by the particular microstate class and therefore portrays how much a particular map is "dominant" compared to all other maps (Koenig et al., 2002, Khanna et al., 2015). We hypothesized that the topography of controls' microstate maps differ from the maps of the patient group, e.g. the landscape of the AD patient's map A might not correspond to the landscape of the control's map A, thus involving comparison of basically different maps and corresponding parameters. Additionally, it has been shown that the usage of the average or mean microstate maps for the between-group comparisons is a valid and reliable approach (Khanna et al., 2014). Therefore, microstate parameters were calculated using the average controls' grand mean maps as the standard that was fitted by spatial correlation to the original patients' EEG data. This procedure allowed for the computation of duration, occurrence and contribution of each healthy elderly microstate map in the patient's EEG data (Fig. 1). The microstate parameters were consequently compared between SCD, MCI and AD groups only.

2.5. Statistical analysis

2.5.1. Microstate statistics

The demographic characteristics, clinical variables (MMSE) and biomarkers (CSF Aβ42, p- and t-tau) of the study population were presented with descriptive statistics. The differences in sex ratio, age, years of education, MMSE and CSF biomarkers between the groups were investigated by Chi Square (sex ratio only) and nonparametric Kruskal-Wallis test, followed by Dunn-Bonferroni test for post-hoc comparisons.

Microstate topographies of each microstate class were compared between healthy controls and patient groups using a non-parametric randomization topographic analysis of variance (TANOVA) (Strik et al., 1998) in the Ragu software (Koenig et al., 2011). The four individual microstate maps per participant, retrieved from the above described cluster analysis and canonical sorting procedure were compared between the four groups (controls, SCD, MCI and AD) in order to identify significant reference-independent topographical differences. Note that the map sorting procedure employed before was designed to minimize the potential variance among microstate maps across individuals and groups, such that these topographic comparisons were as conservative as possible. Post-hoc electrode-wise t-maps were computed between all possible group pairs in case of a significant TANOVA (Controls vs SCD, SCD vs MCI, MCI vs AD, etc.). Both TANOVA and post-hoc tests were conducted after regressing out age and sex, with 5000 randomization runs and level of significance $p < 0.05$.

The group differences in microstate parameters (duration, occurrence and contribution) were investigated using nonparametric Kruskal–Wallis test due to the non-normal distribution of the data. The analysis was performed separately for each microstate parameter. The level of significance was $p < 0.05$.

2.5.2. Correlation of microstates topographies and parameters with clinical variables

The association of the MMSE and CSF biomarkers (Aβ42, p- and t-

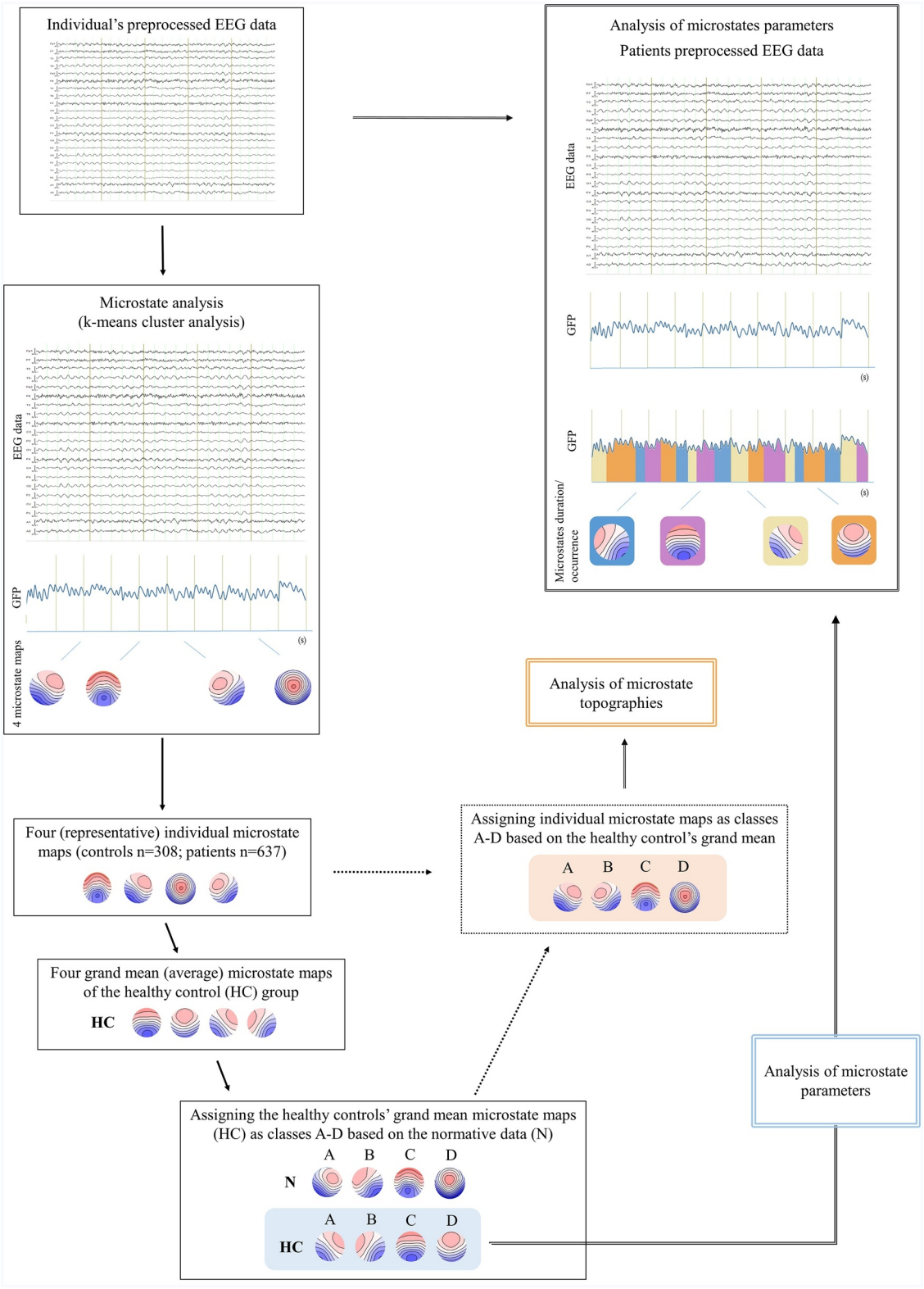

(caption on next page)

Fig. 1. Steps of the EEG microstate analysis. The analysis started with the individual's preprocessed EEG that was subjected to the spatial k-means cluster analysis. The cluster analysis yielded four most representative microstate maps per individual. The next step involved computation of the average or grand mean microstate maps of the healthy elderly group (n = 308). The four healthy grand mean maps were then assigned as class A–D based on the similarity to the maps from the normative study. Following the same sorting procedure, the four individual microstate maps of both healthy controls and patients were assigned (sorted) as class A–D based on the similarity to the four healthy grand mean maps. Finally, sorted and assigned individual microstate maps (orange area) were used for the analysis of their topographical differences between the groups. The healthy controls' grand mean maps (blue area) were further used for the computation of microstate parameters (duration, occurrence and contribution) in the original preprocessed patients' EEG data. HC = grand mean microstate maps of healthy elderly controls, N = average (representative) microstates maps from the normative data (Koenig et al., 2002). (For interpretation of the references to color in this figure legend, the reader is referred to the web version of this article.)

tau; in the memory clinic patient group only) with the topography of microstate classes were investigated using topographic analysis of covariance (TANCOVA). TANCOVA uses nonparametric randomization statistics when the predictor is a continuous variable (Koenig et al., 2011). The data was regressed out for age and sex prior to the analyses. TANCOVAs were separately performed for MMSE and each CSF biomarker, with the 5000 randomization runs.

The correlations of the MMSE (in both healthy and patient groups) and CSF biomarkers (in the patient group) with the microstate parameters were investigated by Spearman's rank correlation tests due to the non-normal distribution of the data.

The level of significance for both TANCOVA and Spearman's correlation tests was $p < 0.05$. All the TANOVA and TANCOVA analyses were conducted in the Ragu software (Koenig et al., 2011). The descriptive statistics, Kruskal-Wallis and Spearman's rank correlation tests were performed in SPSS (SPSS Statistics, version 23.0).

2.6. Data availability statement

Clinical data used in the present study are not publicly available due to the ethical constraints. The researchers interested in the reported findings should contact the study responsible senior (Vesna Jelic, vesna.jelic@ki.se) and corresponding author (Una Smailovic, una.smailovic@ki.se) who will make the data available upon reasonable request. Request for clinical information and data availability of the ongoing longitudinal SNAC-K study (http://www.snac-k.se/) should be directed to Laura Fratiglioni, PI of the SNAC-K study (Laura.Fratiglioni@ki.se). Microstate analysis algorithm and Ragu software have been developed by Thomas König, University of Bern, and are available for downloading online (http://www.thomaskoenig.ch/index.php/software/ragu/download).

3. Results

3.1. Grand mean microstate maps of healthy controls

The descriptive statistics of the study population and CSF biomarkers are presented in Table 1.

The four average or grand mean healthy elderly microstate maps yielded by cluster analysis of the controls' EEGs (n = 308, 60–93 years) were analogous to the four grand mean microstate maps of the normative data published in Koenig et al. (2002) (Fig. 2). The observed differences can be attributed to the age-related changes in microstate topographies as the normative study included only 26 subjects above the age of 50 (Koenig et al., 2002).

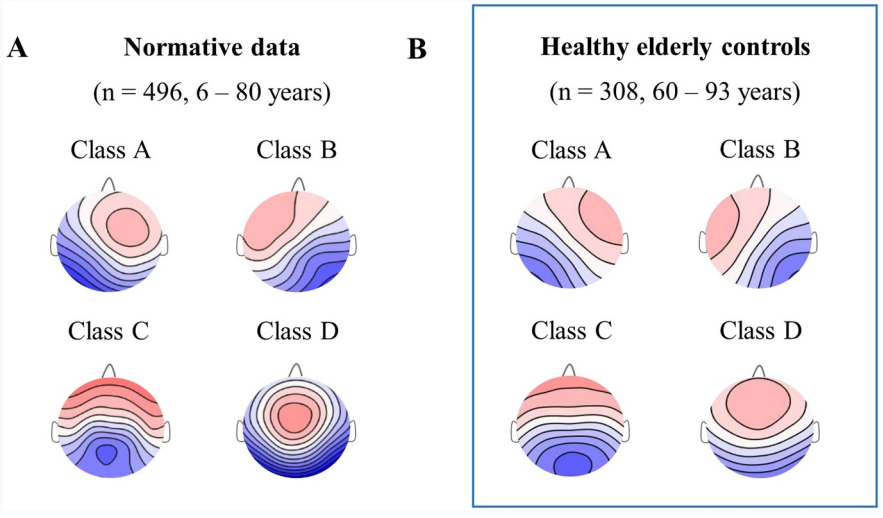

Fig. 2. Microstate maps of the healthy population. Grand mean microstate maps of the (A) Normative data that included 496 controls aged 6 to 80 years but only 26 subjects above the age of 50 (Koenig et al., 2002), (B) Healthy elderly controls included in the present study (n = 308) aged between 60 and 93 years.

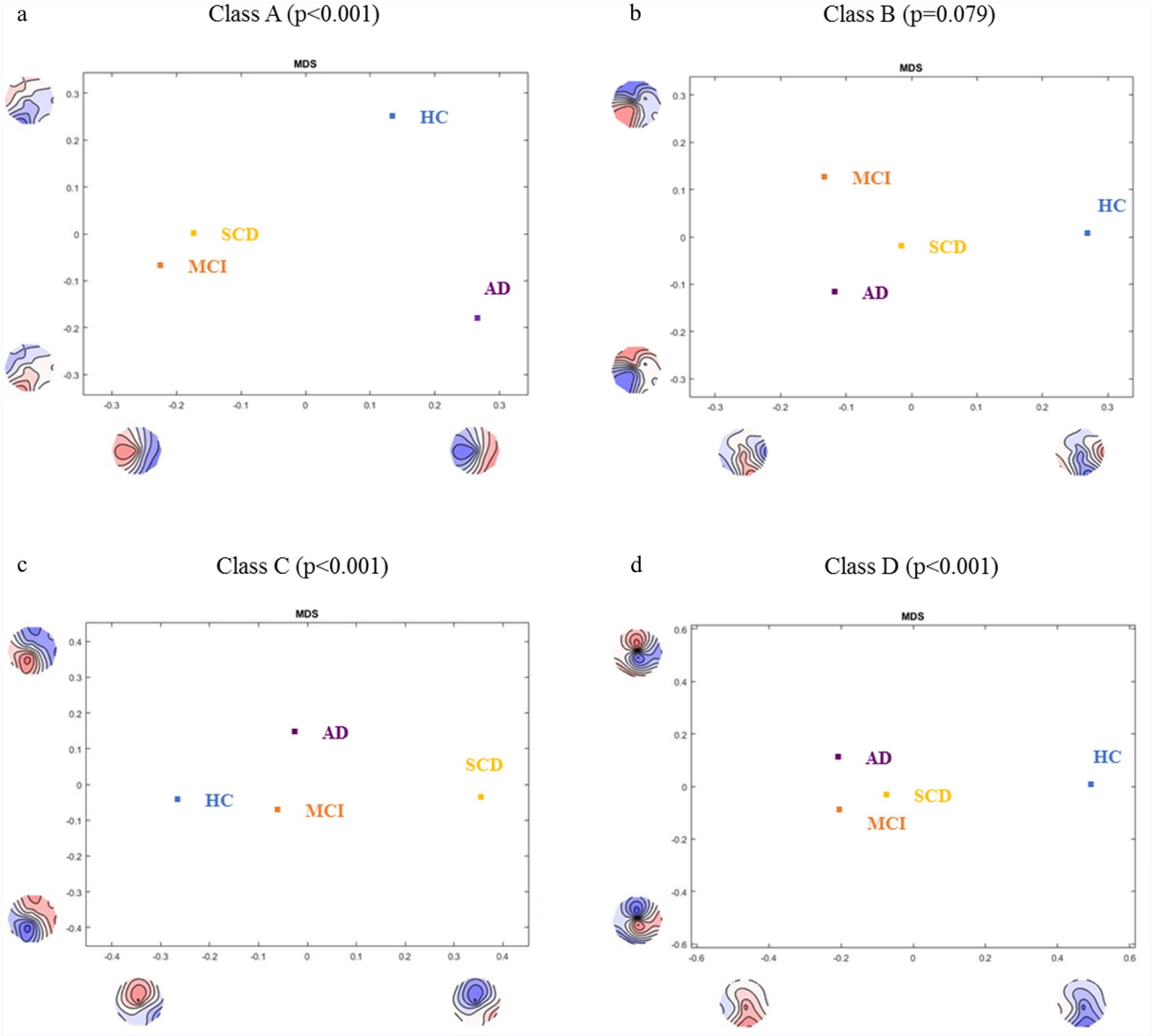

Fig. 3. Analysis of topographical differences in microstate maps. TANOVA of the individual microstate topographies between Controls, SCD, MCI and AD for the microstate class A (a), B (b), C (c) and D (d). The figure displays between-group spatial comparison of each microstate class that has been fed into a multidimensional scaling (MDS) analysis. MDS analysis downscales high-dimensional result spaces into lower dimensional ones by subjecting all mean group maps to the spatial principal component analysis (PCA) that allows visualization of the data. The maps shown on the x- and y-axes represent PCA eigenvector maps. Each group point on the graph is therefore represented in a way that groups with similar topographies will be found at closer whereas groups with dissimilar topographies will be found at the greater mutual distance. HC = healthy elderly controls, SCD = subjective cognitive decline, MCI = mild cognitive impairment, AD = Alzheimer's disease.

3.2. Topographical differences in microstates maps between healthy controls and memory clinic patients

TANOVA showed significant interaction effect of microstate classes * diagnostic groups ($p = 0.027$). TANOVA of the individual microstate topographies revealed significant differences between the healthy elderly controls (HC) and patient groups (SCD, MCI, AD) for microstate classes A, C and D, while controlling for age and sex ($p < 0.001$ for all separate TANOVAs) (Fig. 3). Even though graphical representation of topographical differences suggest deviation of class B in the patient groups, it did not reach statistical significance ($p = 0.079$) (Fig. 3).

Post-hoc tests for the topographical group-wise comparisons

Table 2
Topographical group-wise comparison of microstate maps.

Group pair	A	B	C	D
HC vs SCD	0.011	-	< 0.001	< 0.001
HC vs MCI	0.001	-	n.s.	< 0.001
HC vs AD	0.002	-	n.s.	< 0.001
SCD vs MCI	n.s.	-	0.017	n.s.
SCD vs AD	0.013	-	0.031	n.s.
MCI vs AD	0.006	-	n.s.	n.s.

Post-hoc TANOVA for topographical group-wise comparison of microstate topographies. Microstate maps were corrected for age and sex. Overall TANOVA was significant for maps A, C and D ($p < 0.001$), dash indicates that overall TANOVA was not significant and therefore post-hoc tests were not computed. The table presents p values < 0.05; n.s. = non significant. HC = healthy elderly controls, SCD = subjective cognitive decline, MCI = mild cognitive impairment, AD = Alzheimer's disease.

Table 3
Association of microstate topographies with MMSE and CSF biomarkers.

	A	B	C	D
MMSE (healthy controls)	n.s.	n.s.	n.s.	n.s.
MMSE[1] (patients)	0.027	n.s.	n.s.	n.s.
CSF biomarkers[2]				
CSF Aβ42	n.s.	n.s.	0.049	n.s.
CSF p-tau	n.s.	0.035	n.s.	n.s.
CSF t-tau	n.s.	n.s.	n.s.	n.s.

TANCOVA of the microstate classes with the MMSE and CSF biomarkers as predictors. Analyses controlled for age and sex. The table presents p values < 0.05; n.s. = non significant. MMSE = Mini Mental State Examination. [1] $n = 627$ for the memory clinic cohort (SCD = 206, MCI = 228, AD = 193). [2] $n = 637$, investigated in the patient group only.

between healthy controls and the patient groups revealed statistically significant topographical differences between the maps for microstate classes A (HC vs SCD, $p = 0.011$; HC vs MCI, $p = 0.001$; HC vs AD, $p = 0.002$), C (HC vs SCD, $p < 0.001$) and D (HC vs any of the patient groups, $p < 0.001$). The topographical differences between the patient groups were significant for classes A (SCD vs AD, $p = 0.013$; MCI vs AD, $p = 0.006$) and C (SCD vs MCI, $p = 0.017$; SCD vs AD, $p = 0.031$) (Table 2).

3.3. Association of microstate topography with MMSE and CSF biomarkers

TANCOVA revealed statistically significant association between MMSE score and topography of microstate class A in the patient group only ($p = 0.027$), while controlling for age and sex (Table 3).

The investigation of relationship of microstate class topographies and CSF biomarkers in the patient group revealed statistically significant association between CSF Aβ42 levels and the topography of microstate class C ($p = 0.049$) and CSF p-tau and topography of class B ($p = 0.035$) while controlling for age and sex (Table 3). The direction of topographic deviations in association with MMSE score and CSF biomarkers can be inferred from the covariance maps (Supplementary Fig. 1).

3.4. Differences in microstate parameters between memory clinic patients

The previous analysis revealed significant topographical difference in the microstate maps for classes A, C and D between healthy elderly and the patient groups. Therefore, direct between-group comparison of microstate parameters is confounded by their topographical differences. Consequently, computation of parameters involved fitting of healthy controls average (grand mean) microstate maps onto the original patients EEG recording (SCD, MCI and AD). The four healthy controls microstate maps accounted on average for 78% of the variance in the patients EEG data which is comparable to the literature (Koenig et al., 2002; Michel and Koenig, 2018).

Kruskal–Wallis test revealed statistically longer mean duration in a gradient- like manner between SCD, MCI and AD groups for microstate classes A ($p < 0.001$) and B ($p < 0.001$) . On the other hand, there was statistically significant lower mean occurrence in a gradient-like manner between the SCD, MCI and AD groups in the microstate classes C ($p < 0.001$) and D ($p < 0.001$). Overall, there were significant differences in the mean microstate contribution for all microstates classes (class A, $p = 0.001$; class B, $p < 0.001$; class C, $p = 0.012$; class D, $p = 0.003$). Mean contribution of the asymmetrical (A and B) classes was higher whereas symmetrical (C and D) classes was lower with the more severe stage of cognitive impairment (Fig. 4).

3.5. Association of microstate parameters with MMSE and CSF biomarkers

Spearman correlation revealed significant associations between MMSE, CSF biomarkers values and microstates parameters in the patient cohort, however Spearman's rank coefficient was < 0.25 for all correlations (Supplementary Table 1).

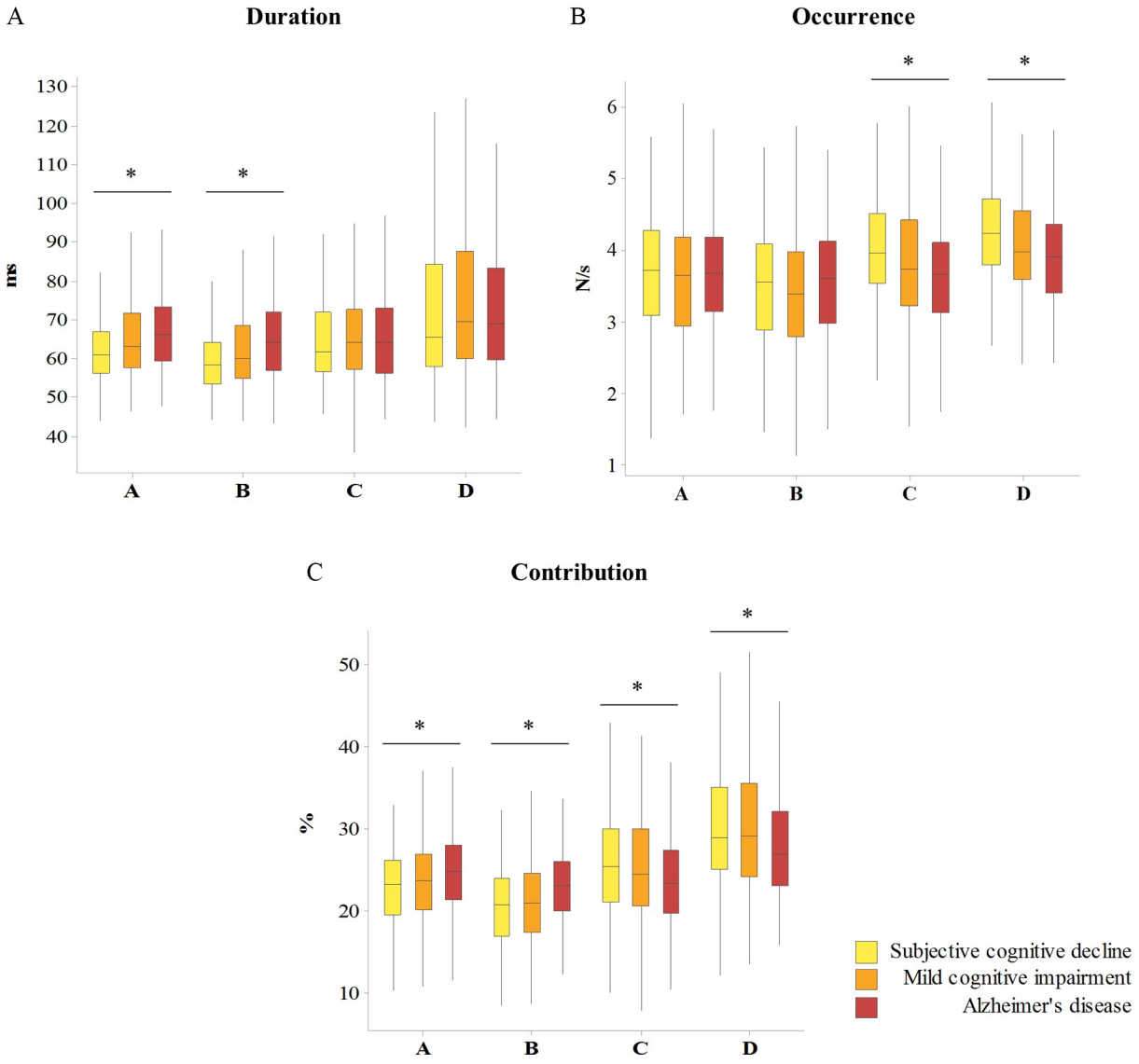

Fig. 4. Gradient-like differences in microstate parameters between memory clinic patient groups. Microstate duration (A), occurrence (B) and contribution (C) between subjective cognitive decline, mild cognitive impairment and Alzheimer's disease patients, using the average (grand mean) maps of the healthy control group for computation. Different bar colors present different diagnostic groups. The interquartile range is presented by the box; the median by the solid line; lower and upper 25% of distribution are presented by whiskers. Kruskal–Wallis test over the diagnostic groups. *$p < 0.05$.

4. Discussion

The present study investigated differences in the topography and dynamics of EEG microstates between the two large and well characterized cohorts of patients with different stages of cognitive impairment and healthy elderly controls. To our knowledge, it is the first EEG study that investigated biological bases of these neurophysiological findings by assessing their relationship with conventional AD molecular markers. In this study we have shown that EEG microstate topographies significantly deviate between the controls, SCD, MCI and AD patients for microstates classes A, C and D. On the one hand, post-hoc group-wise comparisons highlighted that all the patient groups separately (SCD, MCI and AD) had significantly different microstate topographies compared to the healthy controls for classes A and D (Table 2). On the other hand, deviations in the topography of microstates classes C and A might be specific to patients with early (SCD) and advanced (AD) stage of the cognitive impairment, respectively, as supported by the graphical plot of their topographical similarities (Fig. 3) and post-hoc group-wise comparisons (Table 2). These findings indicate the plausible sensitivity of functional microstates to the disturbances in synaptic function and superimposed neural networks that underlie early clinical symptomatology in patients along AD continuum.

A previous EEG study on microstate topographies has demonstrated more frontally located center of gravity of the microstates in patients with AD, however involved obsolete analytical approach (Dierks et al., 1997). Two other studies employing current microstates methodology reported no statistically significant differences in microstate topographies between AD patients and controls; however this might have been due to underpowered analyses given small sample sizes (Nishida et al., 2013; Grieder et al., 2016). The interpretation of deviations in the resting state microstate topographies relies on the concept that different microstate maps mirror different coordinated and synchronized neural networks in the brain. Therefore, changes in the map topographies recorded at the level of the human scalp resemble changes in the activation, distribution and/or orientation of the underlying neural assemblies in the brain (Lehmann et al., 1987; Khanna et al., 2015).

We reported the association between CSF Aβ42 levels and the alterations in the topography of symmetrical microstate class C in the patient cohort. Decreased levels of Aβ42 in the CSF correlate with the increased brain amyloid load evidenced by neuropathological examination or amyloid-positron-emission tomography (PET) (Strozyk et al., 2003; Blennow et al., 2010). Additionally, amyloid cascade hypothesis of AD pathogenesis has dominated the field for several decades (Selkoe and Hardy, 2016), indicating causative relationship between the amyloid accumulation and synaptic dysfunction along AD continuum (Selkoe, 2002; Selkoe and Hardy, 2016). Microstate class C has been previously associated with activation in the parts of the default mode network such as posterior and anterior cingulate cortex as shown by 3D EEG source localization and correlative resting-state fMRI-EEG studies (Britz et al., 2010; Pascual-Marqui et al., 2014; Michel and Koenig, 2018). Concurrently, a recent study aiming to identify spread of AD pathology has shown that earliest Aβ accumulation occurs within areas of default mode network (DMN), affecting functional connectivity of these regions in healthy elderly and MCI patients (Palmqvist et al., 2017). This might explain the reported association between CSF Aβ42 levels and microstate class C since our memory clinic cohort prevalently consisted of patients diagnosed with SCD and MCI. Topographical deviation of microstate map C in patients with cognitive impairment may therefore indicate increased brain amyloid load and consequent functional disruption of the DMN.

On the other hand, we observed significant association of CSF p-tau levels and alterations in the topography of asymmetrical microstate class B. CSF p-tau reflects the phosphorylation state of tau as well as extent of the cortical neurofibrillary tangle pathology (Buerger et al., 2006; Tapiola et al., 2009; Blennow, 2017). Compared to the t-tau levels, it appears to be more specific for AD (Scheurich et al., 2010; Blennow, 2017). Microstate class B has been found to correlate with the bilateral occipital cortex activity as shown by fMRI-EEG study and therefore to be associated with visual network (Britz et al., 2010). Another study, using 3D EEG source localization technique, has shown that class B has a maximum activation in the right occipital area in addition to the posterior cingulate cortex (Pascual-Marqui et al., 2014). Recent reports on brain tau pathology distribution in relation to the resting-state functional neural networks revealed that regional pattern of hyperphosphorylated tau pathology involved temporal cortical areas, precuneus/posterior cingulate, occipital and lateral parietal cortices which corresponds to the dorsal attention, higher visual, limbic and default mode networks (Ossenkoppele et al., 2016; Hansson et al., 2017). Thus, brain areas and networks associated with microstate class B overlap with the regional distribution of hyperphosphorylated tau pathology and consequently affected functional brain networks. Interestingly, topographical differences of class B in our study were not significant between the healthy elderly controls and memory clinic patient groups (Fig. 3). Taking into account that the diagnoses of our memory clinic patients were based on the clinical criteria, we suggest that the deviations in the topography of map B might be a valuable functional marker of the accumulating molecular neuropathology rather than the cognitive status.

Asymmetrical microstate class A and symmetrical class D have been shown to correspond to the resting state networks associated with phonological processing and attention network, respectively (Britz et al., 2010). Conversely, a more recent study reported association of class A with visualization as a modality of thinking, while it confirmed previous finding of association of microstates class D with attention and no-task resting state (Milz et al., 2016). We have reported significant association of MMSE score with the topographical alterations of microstate class A. Even though additional studies are needed to extend and confirm hypothesized topographical and brain network correlates of the microstate maps, the disruptions in default mode network, attention, visual and phonological processing networks have indeed been observed in MCI and AD patients (Sorg et al., 2007; Li et al., 2012; Verma and Howard, 2012; Hafkemeijer et al., 2015; Wang et al., 2015; Badhwar et al., 2017; Mascali et al., 2018).

The microstate parameters analysis showed a significant gradient-like increase in the mean duration of microstate classes A and B and a gradient like decrease in the mean occurrence of classes C and D with the more severe stage of cognitive impairment. The contribution parameter summarizes differences in both duration and occurrence, since it reflects the overall time coverage of a particular map in the whole EEG recording. We reported significant gradient-like increase in mean contributions of asymmetrical classes A and B and decrease in contribution of symmetrical classes C and D with the more severe stage of cognitive impairment.

The same pattern of microstate parameters alterations have already been observed in patients with different stages of cognitive impairment in comparison to the healthy controls (Koenig et al., 2002). Interestingly, this arrangement is exactly the opposite of the one observed during the normal brain development, characterized by decrease in contribution of asymmetrical and increase in contribution of symmetrical microstate classes (Koenig et al., 2002). While the underlying biological substrates of the observed pattern of changes are still open to discussion, these alterations might be related to the broad maturation processes such as myelination and organization of the synaptic connections (Koenig et al., 2002). Besides, one of the observations in the development of the AD neuropathology is that its evolution inversely mirrors development of cortical myelination. In other words, brain areas that are last-to be myelinated are the first to be affected by AD pathology (Braak et al., 1999; Bartzokis, 2004). We therefore hypothesize that described pattern of changes in microstate parameters in patients along AD continuum mirrors progressive region-selective spread of pathology and thus disruption in the impulse transmissions

and functional connectivity of distributed neural networks.

Investigation of the resting states of the brain poses certain advantages in the clinical settings such as straightforward planning and execution, minimal requirements for the patient participation and avoidance of confounding factors such as individual performance on the cognitive tasks (Bressler and Menon, 2010). Therefore, noninvasive and widely accessible resting state EEG might be a method of choice when it comes to the investigation of disruptions in the neurocognitive networks in the preclinical and clinical phases of AD. The present study has however certain limitations, such as lack of direct investigation of correlatives of the EEG microstate topographies with the functional neuroimaging modalities such as fMRI and/or fluorodeoxyglucose-PET (FDG-PET). Longitudinal follow-up of the patients with cognitive impairment would further contribute to the evaluation of prognostic potential of EEG microstate measures. In addition, inclusion of alternative synaptic biomarkers such as novel CSF markers in future studies would substantiate investigation of candidate EEG measures as early markers of synaptic dysfunction along the AD continuum.

4.1. Conclusions

Our results demonstrated extensive relationship of resting state EEG microstates topographies and parameters with the stage of cognitive impairment, MMSE score, CSF Aβ42 and p-tau levels in patients diagnosed with SCD, MCI and AD. EEG microstates might therefore serve as novel functional state and trait markers of brain synchronous activity that contribute to understanding and detecting early disruption of neurocognitive networks in patients along AD continuum.

Declarations of Competing Interest

The authors declare no conflict of interest.

Acknowledgments

This work was supported by European Union's Horizon 2020 research and innovation program under the Marie Sk1odowska-Curie Grant Agreement number 676144 (Synaptic Dysfunction in Alzheimer Disease, SyDAD), Alzheimerfonden and Margaretha af Ugglas Foundation.

The authors would like to thank all the healthy volunteers and memory clinic patients who made this study possible as well as to Thomas Dierks and Milica Gregoric Kramberger for data collection. We thank the participants as well as all staff involved in the data collection and management of the SNAC-K study. SNAC-K is financially supported by the Swedish Ministry of Health and Social Affairs, the participating County Councils and Municipalities, and the Swedish Research Council.

Supplementary materials

Supplementary material associated with this article can be found, in the online version, at doi:10.1016/j.nicl.2019.102046.

References

Badhwar, A, Tam, A, Dansereau, C, Orban, P, Hoffstaedter, F, Bellec, P, 2017. Resting-state network dysfunction in Alzheimer's disease: a systematic review and meta-analysis. Alzheimer's & dementia: diagnosis. Assess. Dis. Monitor. 8, 73–85.

Bartzokis, G., 2004. Age-related myelin breakdown: a developmental model of cognitive decline and Alzheimer's disease. Neurobiol Aging 25 (1), 5–18.

Blennow, K., 2017. A Review of Fluid Biomarkers for Alzheimer's disease: moving from CSF to blood. Neurol. Therapy 6 (Suppl 1), 15–24.

Blennow, K, Hampel, H, Weiner, M, Zetterberg, H, 2010. Cerebrospinal fluid and plasma biomarkers in Alzheimer disease. Nat. Rev. Neurol. 6 (3), 131–144.

Braak, E., Griffing, K., Arai, K., Bohl, J., Bratzke, H., Braak, H., 1999. Neuropathology of Alzheimer's disease: what is new since A. Alzheimer? Eur Arch Psychiatry Clin Neurosci. 249 (3), 14–22.

Bressler, SL, Menon, V., 2010. Large-scale brain networks in cognition: emerging methods and principles. Trends Cogn. Sci. 14 (6), 277–290.

Britz, J, Van De Ville, D, Michel, CM, 2010. BOLD correlates of EEG topography reveal rapid resting-state network dynamics. Neuroimage 52 (4), 1162–1170.

Buerger, K, Ewers, M, Pirttila, T, Zinkowski, R, Alafuzoff, I, Teipel, SJ, et al., 2006. CSF phosphorylated tau protein correlates with neocortical neurofibrillary pathology in Alzheimer's disease. Brain 129 (Pt 11), 3035–3041.

Damoiseaux, JS., 2012. Resting-state fMRI as a biomarker for Alzheimer's disease? Alzheimer's Res. Therapy 4 (2), 13848–13853.

Dierks, T, Jelic, V, Julin, P, Maurer, K, Wahlund, LO, Almkvist, O, et al., 1997. EEG-microstates in mild memory impairment and Alzheimer's disease: possible association with disturbed information processing. J Neural Transm (Vienna) 104 (4-5), 483–495.

Efron, R., 1970. The minimum duration of a perception. Neuropsychologia 8 (1), 57–63.

Engels, MMA, Stam, CJ, van der Flier, WM, Scheltens, P, de Waal, H, van Straaten, ECW, 2015. Declining functional connectivity and changing hub locations in Alzheimer's disease: an EEG study. BMC Neurol. 15, 145.

Grieder, M, Koenig, T, Kinoshita, T, Utsunomiya, K, Wahlund, LO, Dierks, T, et al., 2016. Discovering EEG resting state alterations of semantic dementia. Clin. Neurophysiol. 127 (5), 2175–2181.

Hafkemeijer, A, Möller, C, Dopper, E, Jiskoot, L, Schouten, T, van Swieten, J, et al., 2015. Resting state functional connectivity differences between behavioral variant frontotemporal dementia and Alzheimer's disease. Front. Hum. Neurosci. 9 (474).

Hansson, O, Grothe, MJ, Strandberg, TO, Ohlsson, T, Hägerström, D, Jögi, J, et al., 2017. Tau pathology distribution in Alzheimer's disease corresponds differentially to cognition-relevant functional brain networks. Front. Neurosci. 11, 167.

He, BJ, Shulman, GL, Snyder, AZ, Corbetta, M, 2007. The role of impaired neuronal communication in neurological disorders. Curr. Opin. Neurol. 20 (6), 655–660.

Huang, C, Wahlund, L, Dierks, T, Julin, P, Winblad, B, Jelic, V, 2000. Discrimination of Alzheimer's disease and mild cognitive impairment by equivalent EEG sources: a cross-sectional and longitudinal study. Clin. Neurophysiol. 111 (11), 1961–1967.

Ihl, R, Dierks, T, Froelich, L, Martin, E, Maurer, K, 1993. Segmentation of the Spontaneous EEG in Dementia of the Alzheimer type. Neuropsychobiology 27 (4), 231–236.

Jelic, V, Shigeta, M, Julin, P, Almkvist, O, Winblad, B, Wahlund, LO, 1996. Quantitative electroencephalography power and coherence in Alzheimer's disease and mild cognitive impairment. Dementia 7 (6), 314–323.

Jessen, F, Amariglio, RE, Boxtel, M, Breteler, M, Ceccaldi, M, Chételat, G, 2014. A conceptual framework for research on subjective cognitive decline in preclinical Alzheimer's disease. Alzheimers Dement 10 (6), 844–852.

Jessen, F, Wiese, B, Bachmann, C, Eifflaender-Gorfer, S, Haller, F, Kolsch, H, et al., 2010. Prediction of dementia by subjective memory impairment: effects of severity and temporal association with cognitive impairment. Arch. Gen. Psychiatry 67 (4), 414–422.

Khanna, A, Pascual-Leone, A, Farzan, F, 2014. Reliability of Resting-State Microstate Features in Electroencephalography. PLoS One 9 (12), e114163.

Khanna, A, Pascual-Leone, A, Michel, CM, Farzan, F, 2015. Microstates in resting-State EEG: current status and future directions. Neurosci. Biobehav. Rev. 0, 105–113.

Koenig, T, Kottlow, M, Stein, M, Melie-Garcia, L, 2011. Ragu: a free tool for the analysis of EEG and MEG event-related scalp field data using global randomization statistics. Comput. Intell. Neurosci., 938925.

Koenig, T, Prichep, L, Dierks, T, Hubl, D, Wahlund, LO, John, ER, et al., 2005. Decreased EEG synchronization in Alzheimer's disease and mild cognitive impairment. Neurobiol. Aging 26 (2), 165–171.

Koenig, T, Prichep, L, Lehmann, D, Sosa, PV, Braeker, E, Kleinlogel, H, et al., 2002. Millisecond by millisecond, year by year: normative EEG microstates and developmental stages. Neuroimage 16 (1), 41–48.

Lehmann, D, Ozaki, H, Pal, I, 1987. EEG alpha map series: brain micro-states by space-oriented adaptive segmentation. Electroencephalogr. Clin. Neurophysiol. 67 (3), 271–288.

Lehmann, D, Pascual-Marqui, RD, Strik, WK, Koenig, T, 2010. Core networks for visual-concrete and abstract thought content: a brain electric microstate analysis. Neuroimage 49 (1), 1073–1079.

Lehmann, D, Strik, WK, Henggeler, B, Koenig, T, Koukkou, M, 1998. Brain electric microstates and momentary conscious mind states as building blocks of spontaneous thinking: I. Visual imagery and abstract thoughts. Int. J. Psychophysiol. 29 (1), 1–11.

Leuchter, AF, Newton, TF, Cook, IA, Walter, DO, Rosenberg-Thompson, S, Lachenbruch, PA, 1992. Changes in brain functional connectivity in Alzheimer-type and multi-infarct dementia. Brain 115 (5), 1543–1561.

Li, R, Wu, X, Fleisher, AS, Reiman, EM, Chen, K, Yao, L, 2012. Attention-related networks in Alzheimer's disease: a resting functional MRI study. Hum. Brain Mapp. 33 (5), 1076–1088.

Li, SJ, Li, Z, Wu, G, Zhang, MJ, Franczak, M, Antuono, PG, 2002. Alzheimer disease: evaluation of a functional MR imaging index as a marker. Radiology 225 (1), 253–259.

Mascali, D, DiNuzzo, M, Serra, L, Mangia, S, Maraviglia, B, Bozzali, M, et al., 2018. Disruption of semantic network in mild Alzheimer's disease revealed by resting-state fMRI. Neuroscience 371, 38–48.

Michel, CM, 2009. Electrical Neuroimaging. Cambridge University Press, Cambridge.

Michel, CM, Koenig, T., 2018. EEG microstates as a tool for studying the temporal dynamics of whole-brain neuronal networks: a review. Neuroimage 180, 577–593.

Milz, P, Faber, PL, Lehmann, D, Koenig, T, Kochi, K, Pascual-Marqui, RD, 2016. The functional significance of EEG microstates-Associations with modalities of thinking. Neuroimage 125, 643–656.

Morrison, JH, Rogers, J, Scherr, S, Levis, DA, Campbell, MJ, Bloom, FE, et al., 1996. The Laminar and Regional Distribution Of Neocortical Somatostatin and Neuritic Plaques: Implications for Alzheimer's Disease as a Global Neocortical Disconnection Syndrome. Academic Press, Orlando.

Musso, F, Brinkmeyer, J, Mobascher, A, Warbrick, T, Winterer, G, 2010. Spontaneous

brain activity and EEG microstates. A novel EEG/fMRI analysis approach to explore resting-state networks. Neuroimage 52 (4), 1149–1161.
Nishida, K, Morishima, Y, Yoshimura, M, Isotani, T, Irisawa, S, Jann, K, et al., 2013. EEG microstates associated with salience and frontoparietal networks in frontotemporal dementia, schizophrenia and Alzheimer's disease. Clin. Neurophysiol. 124 (6), 1106–1114.
Olsson, A, Vanderstichele, H, Andreasen, N, De Meyer, G, Wallin, A, Holmberg, B, et al., 2005. Simultaneous measurement of beta-amyloid(1-42), total tau, and phosphorylated tau (Thr181) in cerebrospinal fluid by the xMAP technology. Clin. Chem. 51 (2), 336–345.
Ossenkoppele, R, Schonhaut, DR, Scholl, M, Lockhart, SN, Ayakta, N, Baker, SL, et al., 2016. Tau PET patterns mirror clinical and neuroanatomical variability in Alzheimer's disease. Brain 139 (5), 1551–1567.
Palmqvist, S, Schöll, M, Strandberg, O, Mattsson, N, Stomrud, E, Zetterberg, H, et al., 2017. Earliest accumulation of β-amyloid occurs within the default-mode network and concurrently affects brain connectivity. Nat. Commun. 8 (1), 1214.
Park, Y-M, Che, H-J, Im, C-H, Jung, H-T, Bae, S-M, Lee, S-H, 2008. Decreased EEG synchronization and its correlation with symptom severity in Alzheimer's disease. Neurosci. Res. 62 (2), 112–117.
Pascual-Marqui RD, Lehmann D, Faber PL, Milz P, Kochi K, Yoshimura M, et al. The Resting Microstate Networks (RMN): cortical distributions, dynamics, and frequency specific information flow. arXiv:141119492014.
Pascual-Marqui, RD, Michel, CM, Lehmann, D, 1995. Segmentation of brain electrical activity into microstates: model estimation and validation. IEEE Trans. Biomed. Eng. 42 (7), 658–665.
Raichle, ME., 2010. Two views of brain function. Trends Cogn. Sci. 14 (4), 180–190.
Raichle, ME, MacLeod, AM, Snyder, AZ, Powers, WJ, Gusnard, DA, Shulman, GL, 2001. A default mode of brain function. Proc. Natl. Acad. Sci. USA 98 (2), 676–682.
Scheurich, A, Urban, PP, Koch-Khoury, N, Fellgiebel, A, 2010. CSF phospho-tau is independent of age, cognitive status and gender of neurological patients. J. Neurol. 257 (4), 609–614.
Seeley, WW, Crawford, RK, Zhou, J, Miller, BL, Greicius, MD, 2009. Neurodegenerative diseases target large-scale human brain networks. Neuron 62 (1), 42–52.
Selkoe, DJ., 2002. Alzheimer's disease is a synaptic failure. Science 298 (5594), 789–791.
Selkoe, DJ, Hardy, J., 2016. The amyloid hypothesis of Alzheimer's disease at 25 years. EMBO Mol. Med. 8 (6), 595–608.
Smailovic, U, Koenig, T, Kareholt, I, Andersson, T, Kramberger, MG, Winblad, B, et al., 2018. Quantitative EEG power and synchronization correlate with Alzheimer's disease CSF biomarkers. Neurobiol. Aging 63, 88–95.
Sorg, C, Riedl, V, Mühlau, M, Calhoun, VD, Eichele, T, Läer, L, et al., 2007. Selective changes of resting-state networks in individuals at risk for Alzheimer's disease. Proc. Natl. Acad. Sci. 104 (47), 18760.
Stevens, A, Kircher, T., 1998. Cognitive decline unlike normal aging is associated with alterations of EEG temporo-spatial characteristics. Eur. Arch. Psychiatry Clin. Neurosci. 248 (5), 259–266.
Strik, WK, Chiaramonti, R, Muscas, GC, Paganini, M, Mueller, TJ, Fallgatter, AJ, et al., 1997. Decreased EEG microstate duration and anteriorisation of the brain electrical fields in mild and moderate dementia of the Alzheimer type. Psychiatry Res. 75 (3), 183–191.
Strik, W.K., Fallgatter, A.J., Brandeis, D., Pascual-Marqui, R.D., 1998. Three-dimensional tomography of event-related potentials during response inhibition: evidence for phasic frontal lobe activation. Electroencephalogr Clin Neurophysiol. 108 (4), 406–413.
Strozyk, D, Blennow, K, White, LR, Launer, LJ, 2003. CSF Abeta 42 levels correlate with amyloid-neuropathology in a population-based autopsy study. Neurology 60 (4), 652–656.
Tapiola, T, Alafuzoff, I, Herukka, SK, Parkkinen, L, Hartikainen, P, Soininen, H, et al., 2009. Cerebrospinal fluid beta-amyloid 42 and tau proteins as biomarkers of Alzheimer-type pathologic changes in the brain. Arch. Neurol. 66 (3), 382–389.
Varela, F, Lachaux, J-P, Rodriguez, E, Martinerie, J, 2001. The brainweb: phase synchronization and large-scale integration. Nat. Rev. Neurosci. 2, 229–239.
Verma, M, Howard, RJ., 2012. Semantic memory and language dysfunction in early Alzheimer's disease: a review. Int. J. Geriatr. Psychiatry 27 (12), 1209–1217.
Wang, P, Zhou, B, Yao, H, Zhan, Y, Zhang, Z, Cui, Y, et al., 2015. Aberrant intra- and inter-network connectivity architectures in Alzheimer's disease and mild cognitive impairment. Sci. Rep. 5, 14824.
Winblad, B, Palmer, K, Kivipelto, M, Jelic, V, Fratiglioni, L, Wahlund, LO, et al., 2004. Mild cognitive impairment-beyond controversies, towards a consensus: report of the International Working Group on Mild Cognitive Impairment. J. Intern. Med. 256 (3), 240–246.
Organization, World Health, 1992. The ICD-10 Classification of Mental and Behavioural Disorders: Clinical Descriptions and Diagnostic Guidelines Geneva.
Yuan, H, Zotev, V, Phillips, R, Drevets, WC, Bodurka, J, 2012. Spatiotemporal dynamics of the brain at rest - Exploring EEG microstates as electrophysiological signatures of BOLD resting state networks. Neuroimage 60 (4), 2062–2072.